

# Super-Arrhenius behaviour of molecular glass formers

Ankit Singh and Yashwant Singh

*Department of Physics, Banaras Hindu University, Varanasi-221 005, India.*

(Dated: February 5, 2019)

A theory is developed to calculate values of the potential energy barriers to structural relaxation in molecular glass formers from the data of static pair correlation function. The barrier height is shown to increase due to increase in number of the “stable bonds” a particle forms with its neighbours and energy of each bond as liquids move deeper into the supercooled (supercompressed) region. We present results for a system of hard-spheres and compare calculated values of the structural relaxation time with experimental and simulation results.

PACS numbers: 64.70.Q-, 61.20.Gy, 64.70.kj

The structural relaxation time of a molecular glass former grows by many orders of magnitude over a small range of temperatures when the system is cooled close to the glass transition temperature [1]. The glass transition is linked to dynamical arrest caused by particles being trapped in cages formed by their nearest neighbours [2, 3]. It is widely accepted that the dynamics close to the glass transition is dominated by activation [4]. If the potential energy barriers to relaxation were constant in temperatures, the relaxation time would follow the Arrhenius law. The super-Arrhenius behaviour suggests that the potential energy barriers in molecular glass formers increase with decreasing temperature and increasing density. The ubiquity of the phenomenon, irrespective of molecular details points to a collective or cooperative behaviour characterized by a length scale that grows as one approaches to the glass transition. Beginning at least from Adam and Gibbs [5] who introduced the concept of “cooperatively rearranging regions” in the mid - 1960’s, many microscopic models [6–11] have been developed to uncover the physical mechanism behind growth of the cooperative length scale. One of the issues has been to define and determine objectively such a length scale [10–12], and relate it with the potential energy barrier.

In dealing with classical many-body particle systems one often integrates out kinetic energy of particles and considers only potential energy of interactions in framing a theory or in simulations. In this letter we show that when kinetic energy is allowed to compete with effective potential energy felt by particles in a system, a new way of understanding properties of dense systems emerges. Such an idea was first proposed by Hill [13] and used by Stogryn and Hirschfelder [14] and others [15] to describe equilibrium and transport properties of gases.

A particle in a dense system feels potential energy barrier created by its neighbours. Depending upon height of the barrier and the relative momenta of surrounding particles, the central particle may get trapped and bonded (defined below) with neighbouring particles. A particle whose total energy is higher than the barrier moves freely and collides with other particles. The concentration of these particles depends on density and temperature; the potential barrier becomes higher on increasing the density and lowering the temperature and kinetic energy of

particles decreases on decreasing the temperature. A molecular liquid at high densities and low temperatures can therefore be considered as a network of particles connected with each other by (non-chemical) bonds with some free particles which move around and collide with other particles. Depending upon bonding energies, the life time of bonds may vary from microscopic to macroscopic time. When a particle dissociates from the network either by collision or by thermal activation, it may initiate breaking of neighbouring bonds and creating a dynamical active domain [16, 17]. The precipitous onset of slowness can be associated with increasing number of bonds and the larger bond energy with which particles are bonded with neighbours.

One way to find number of bonds formed by a particle with its neighbours is to use data of static pair correlation function. The theory we describe is applicable to all those systems for whose values of pair correlation function in supercooled (super-compressed) region are available. Here we consider a system of hard spheres and use data of the radial distribution function (RDF) evaluated from an approximate integral equation theory [18] (our aim here is to show usefulness of the theory rather than numerical rigour).

In case of a system of hard-spheres where potential is zero when particles do not overlap and infinite otherwise, temperature becomes irrelevant apart from rescaling quantities, the natural control parameter is the packing fraction  $\eta = \frac{\pi}{6}\rho\sigma^3$ , where  $\rho$  is number density and  $\sigma$  particles diameter. Experimentally, hard-sphere systems are obtained using colloidal particles [19], emulsions, or granular materials [20]. The fluid-crystal transition takes place at  $\eta = 0.494$  and the melting transition at  $\eta = 0.545$ . When the system is compressed following a protocol which avoids crystallization, the structural relaxation time  $\tau_\alpha$  increases rapidly showing super-Arrhenius behaviour. Whether  $\tau_\alpha$  diverges at a density lower than the random close packed density,  $\eta_{rcp} (\simeq 0.64)$  or not is still a highly debated issue [21–23]. Kinetic arrest must occur at  $\eta_{rcp}$  because all particles block each other at that density.

The RDF  $g(r)$  of a homogeneous and isotropic system consisting of particles of mass  $m$  in the centre of mass coordinates can be written as

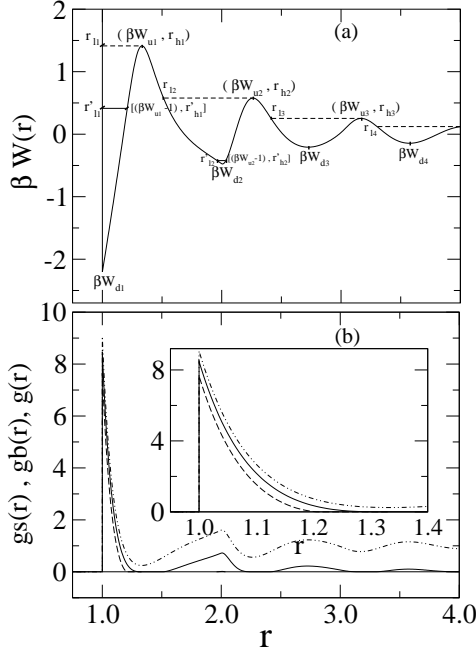


FIG. 1. (a). The reduced effective potential  $\beta W(r)$  between a pair of particles separated by distance  $r$  (expressed in unit of hard-spheres diameter  $\sigma$ ) in a system of hard-spheres at a packing fraction  $\eta = 0.59$ .  $\beta W_{ui}, r_{hi}$  are, respectively, value and location of  $i^{th}$  maximum and  $r_{li}$  is the location on the left hand side of the shell where  $\beta W_i(r) = \beta W_{ui}$  (shown by dashed line). The location  $r'_{li}$  and  $r'_{hi}$  are values of  $r$  on the left and the right hand side of the shell where  $\beta W_i(r) = \beta W_{ui} - 1$  (shown by full line).  $\beta W_{di}$  is the depth of the  $i^{th}$  shell. (b). Radial distribution functions  $g(r)$  (dash-dotted line),  $g_b(r)$  (full line) and  $g_s(r)$  (dashed line) vs  $r$  at  $\eta = 0.59$ . The various peaks correspond to various shells around a central particle. While  $g(r)$  oscillates around one,  $g_b(r)$  and  $g_s(r)$  become zero at boundaries defined by  $(r_{li}, r_{hi})$  for  $g_b(r)$  and  $(r'_{li}, r'_{hi})$  for  $g_s(r)$ . In the inset we show how values in the first shell differ from each other.

$$g(r) = \left( \frac{\beta}{2\pi\mu} \right)^{\frac{3}{2}} \int d\mathbf{p} e^{-\beta(\frac{p^2}{2\mu} + W(r))}, \quad (1)$$

where  $\beta = (k_B T)^{-1}$  is the inverse temperature measured in unit of the Boltzmann constant  $k_B$  and  $\mathbf{p}$  is the relative momentum of a particle of mass  $\mu = m/2$ . The effective potential  $W(r) = -k_B T \ln g(r)$  [24] is sum of the (bare) pair potential and the system induced potential energy of interaction between a pair of particles separated by distance  $r$ . In Fig. 1 we plot  $\beta W(r)$  for a system of hard spheres at  $\eta = 0.59$  as a function of  $r$  expressed in unit of  $\sigma$ . The curve has several maxima and minima. We denote a region between two maxima  $i-1$  and  $i$  ( $i \geq 1$ ) as  $i^{th}$  shell and the minimum of the shell by  $\beta W_{di}$ . The value of  $i^{th}$  maximum is denoted by  $\beta W_{ui}$  and its location by  $r_{hi}$ .

All particles of  $i^{th}$  shell whose energies are less or equal to  $\beta W_{ui}$  i.e;  $\beta(\frac{p^2}{2\mu} + W_i(r)) \leq \beta W_{ui}$  get confined in the

shell and can be considered to be bonded with the central particle. The contribution made to  $g(r)$  by these particles is

$$\begin{aligned} g_{bi}(r) &= 4\pi \left( \frac{\beta}{2\pi\mu} \right)^{\frac{3}{2}} e^{-\beta W_i(r)} \int_0^{\sqrt{2\mu(W_{ui} - W_i(r))}} e^{-\frac{\beta p^2}{2\mu}} p^2 dp \\ &= e^{-\beta W_i(r)} \frac{\Gamma(\frac{3}{2}, \beta(W_{ui} - W_i(r)))}{\Gamma(\frac{3}{2})}, \end{aligned} \quad (2)$$

where  $\Gamma(m, n)$  is the incomplete gamma function and  $W_i(r)$  is the effective potential of  $i^{th}$  shell in the range  $r_{li} \leq r \leq r_{hi}$ . Here  $r_{li}$  is the value of  $r$  where  $\beta W_i(r_{li}) = \beta W_{ui}$  on the left hand side of the shell (see Fig. 1). In Fig. 1(b) we plot  $g(r)$  and  $g_b(r)$  as a function of  $r$  at  $\eta = 0.59$ . The number of bonded particles of  $i^{th}$  shell at packing fraction  $\eta$  is

$$n_{bi}(\eta) = 24\eta \int_{r_{li}}^{r_{hi}} g_{bi}(r) r^2 dr. \quad (3)$$

The total number of particles bonded with the central particle is  $N_b(\eta) = \sum_i n_{bi}(\eta)$ . As shown in Fig. 2(a) by full line,  $N_b$  increases rapidly above the freezing density. This is due to increase in number of shells that surround the central particle and values of  $\beta W_{ui}$  and  $\beta W_{di}$  with  $\eta$ . It may, however be noted that these particles (or bonds) are embedded in a system which is equipped with thermal energy  $k_B T$ . Therefore, all those particles whose energies lie between  $\beta W_{ui} - 1$  and  $\beta W_{ui}$  may not remain bonded for long due to thermal fluctuations; the life time depends on the bonding energy. We call these particles meta-stably bonded (henceforth referred to as m-particles) and those particles whose energies lie between  $\beta W_{di}$  and  $\beta W_{ui} - 1$ , stably bonded (henceforth referred to as s-particles). Most particles of  $N_b$  shown in Fig. 2(a) surrounding the central particle over a length of the pair correlation function are m-particles with bond energies much smaller than the thermal energy and are therefore transient.

The contribution made to  $g(r)$  by the s-particles of  $i^{th}$  shell is

$$g_{si}(r) = 4\pi \left( \frac{\beta}{2\pi\mu} \right)^{\frac{3}{2}} e^{-\beta W_i(r)} \int_0^{\sqrt{2\mu(W_{ui} - K_B T - W_i(r))}} e^{-\frac{\beta p^2}{2\mu}} p^2 dp, \quad (4)$$

where  $W_i(r)$  is in the range,  $r'_{li} \leq r \leq r'_{hi}$ . Here  $r'_{li}$  and  $r'_{hi}$  are respectively, values of  $r$  on the left and the right hand side of the shell where  $\beta W_i(r) = \beta W_{ui} - 1$  (see Fig. 1). We show values of  $g_s(r)$  vs  $r$  in Fig. 1(b) by dashed line for  $\eta = 0.59$ . The number of s-particles with which central particle is bonded, is

$$N_s(\eta) = \sum_i n_{si}(\eta); \quad n_{si}(\eta) = 24\eta \int_{r'_{li}}^{r'_{hi}} g_{si}(r) r^2 dr. \quad (5)$$

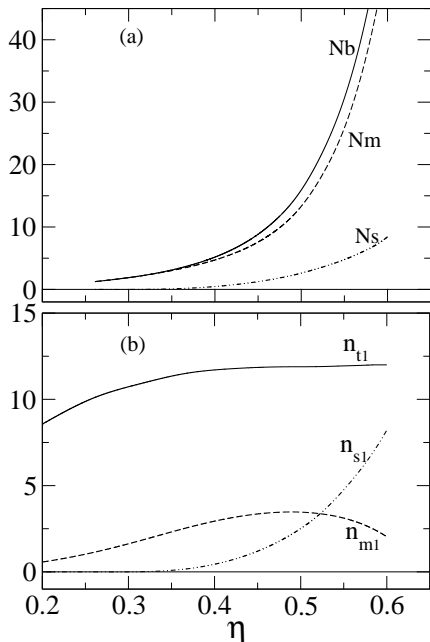


FIG. 2. (a). Number of total bonds  $N_b$ , metastable bonds  $N_m$  and stable bonds  $N_s$  formed by a particle in a system of hard-spheres vs packing fraction  $\eta$ .

(b). Number of total particles  $n_{t1}$ , metastably bonded particles (m-particles)  $n_{m1}$  and stably bonded particles (s-particles)  $n_{s1}$  in the first shell. The number  $n_{s1}$  increases rapidly and crosses  $n_{m1}$  at  $\eta \simeq 0.524$ . At  $\eta = 0.524$  the crossover from nonactivated to activated dynamics takes place, due to formation of cage by s-particles.

We plot,  $N_s$  vs  $\eta$  in Fig. 2(a) along with  $N_b$  and  $N_m = (N_b - N_s)$ .

To understand why above a certain density a particle gets trapped by a stiff barrier and there is a crossover from nonactivated to activated dynamics, we examine the nature of particles of the first shell surrounding the central particle as function of  $\eta$ . In Fig. 2(b) we plot number of total particles  $n_{t1}$ , m-particles  $n_{m1}$  and s-particles  $n_{s1}$ . We note that  $n_{t1}$  reaches the maximum value 12 at a density lower than the freezing density where most particles are still free. The number of m-particles  $n_{m1}$  first increases and after reaching a maximum value ( $\simeq 3$ ) at  $\eta \simeq 0.50$  starts decreasing and crosses  $n_{s1}$  at  $\eta \simeq 0.524$ . The number of s-particles ( $n_{s1}$ ) which build up the potential energy barrier increases rapidly on increasing the density. We therefore consider  $\eta = 0.524$  as the density which separates the two distinct dynamical domains. As for  $\eta < 0.524$  the potential barrier is inconsequential the activation is not main mechanism of relaxation; the dynamics can be described by the mode coupling theory (MCT) [25]. The activated dynamics becomes dominant for  $\eta \geq 0.524$  when the central particle gets surrounded by increasing number of s-particles and the barrier starts caging the particle.

The potential energy barrier to relaxation (activation energy) is assumed to be equal to the energy with which

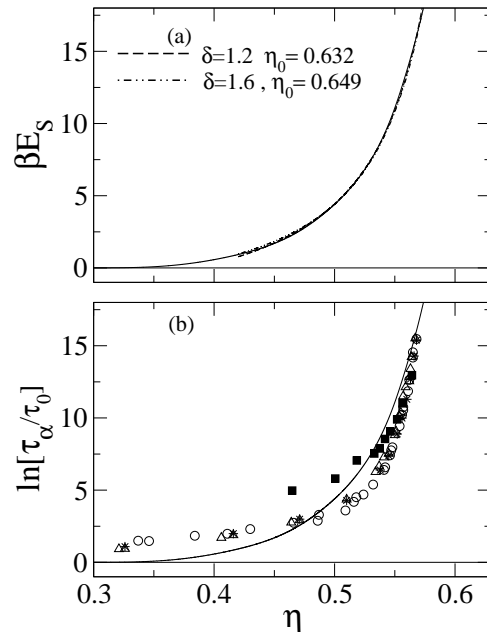


FIG. 3. (a). The potential energy barrier (activation energy)  $\beta E_s$  vs  $\eta$ . Values found from the expression  $\beta E_s(\eta) = A + \frac{B}{(\eta_0 - \eta)^\delta}$  with (i)  $\delta = 1.2, \eta_0 = 0.632$  (dashed line) and (ii)  $\delta = 1.6, \eta_0 = 0.649$  (dash-dotted line) are compared with the calculated values.

(b). Calculated values (solid line) of  $\ln[\frac{\tau_\alpha}{\tau_0}]$  are compared with experimental values (filled square [26] and open circles [27]) and simulation values (open triangles [27] and stars [28]). The values of refs. [27] and [28] are shifted to lower density by an amount  $\Delta\eta = 0.03$ .

a particle is bonded with s-particles. Thus the activation energy,

$$\beta E_s(\eta) = 24\eta \sum_i \int_{r'_{i1}}^{r'_{hi}} (\beta W_{ui} - \beta W_i(r)) g_{si}(r) r^2 dr. \quad (6)$$

Here the bonding energy of each bond is measured from the barrier height.

In Fig. 3(a) we plot  $\beta E_s(\eta)$  vs  $\eta$  and note that  $\beta E_s$  increases sharply for  $\eta > 0.524$ . The energy  $\beta E_s$  can be considered as the activation energy in the Arrhenius law,  $\tau_\alpha(\eta) = \tau_0 \exp(\beta E_s(\eta))$  where  $\tau_0$  is a microscopic time scale. Out of different functional forms used to fit the data of  $\beta E_s(\eta)$ , the best fit was found for  $\beta E_s(\eta) = A + \frac{B}{(\eta_0 - \eta)^\delta}$ . In Fig. 3(a) we compare values found with (i)  $\delta = 1.2, \eta_0 = 0.632$  and (ii)  $\delta = 1.6, \eta_0 = 0.649$ ; though both sets give equally good fit but while one set gives value of  $\eta$  where  $\tau_\alpha$  diverges, lower, the other higher than  $\eta_{rcp}$  ( $= 0.64$ ) indicating limitation of such fitting. We emphasize that the fit shown in Fig. 3(a) not necessarily favours the Vogel-Fulcher-Tammann (VFT) law over other laws of relaxation as the low density data where nonactivated dynamics mainly contributes to relaxations are not included in the fitting.

In Fig. 3(b) we compare our results of  $\tau_\alpha$  with experimental results reported for colloidal hard spheres in refs. [26], [27] and simulation results reported in ref. [28]. It may, however, be noted that while our result is for a monodisperse system, the simulation result [28] is for a 50:50 binary mixture with diameters  $\sigma$  and  $1.4\sigma$  and the experimental results are for polydisperse systems with polydispersity,  $s$ , of about 6% in [26] and above 10% in [27]. From simulation studies [29–31] it has been found that while moderately disperse hard spheres ( $s \sim 5-6\%$ ) behave almost like a monodisperse system, systems with larger dispersity ( $s \gtrsim 10\%$ ) behave in a complex way. One such effect is to move the glass transition to higher  $\eta$ . The unusual aging behaviour due to strong decoupling between small and large spheres for  $\eta > 0.59$  has also been observed [31, 32]. The experimental [27] and simulation [27, 28] data plotted in Fig. 3(b) are shifted to lower density by an amount  $\Delta\eta = 0.03$ , whereas the experimental values taken from ref. [26] are plotted (shown by filled square) without any shift. It may be noted that while the shifted values of refs. [27] and [28] are in good agreement with values of ref. [26] for  $\eta > 0.53$ , considerable difference remains in their values for  $\eta < 0.53$ . This suggests the need for more experimental data of moderately disperse systems [33]. The theoretical values shown

by full line in the figure is in good agreement with these data for  $\eta \gtrsim 0.50$ ; agreement for  $\eta \lesssim 0.50$  is not expected as dynamics in this region as argued above, is other than activation which has not been considered.

In summary: We developed a theory to calculate the potential energy barriers to structural relaxation in a molecular glass formers from the data of static pair correlation function. A particle in a molecular liquid in the supercooled (supercompressed) region gets localized by forming (nonchemical) “stable bonds” with neighbouring particles. The number of bonds and the bonding energy increase on lowering the temperature and increasing the density. The barrier height (activation energy) is equal to the energy  $\beta E_s$  with which a particle is bonded with the s-particles. When  $\beta E_s$  is substituted in the Arrhenius law, a super-Arrhenius feature emerges. Using values of the radial distribution function for a system of hard spheres found from an approximate integral equation theory [18] we calculated the activation energy. The calculated values of  $\tau_\alpha$  is found to be in agreement with the experimental and simulation data in the region where activated dynamics is dominant.

We acknowledge financial help from the Council of Scientific and Industrial Research and the Indian National Science Academy, New Delhi.

- 
- [1] C. A. Angell, *Science* **267**, 1924 (1995); P. G. Debenedetti and F. H. Stillinger, *Nature (London)* **410**, 259 (2001).
- [2] W. K. Kegel and A. van Blaaderen, *Science* **287**, 290 (2000).
- [3] Z. Brown, M. J. Iwanicki, M. D. Gratale, X. Ma, A.G. Yodh, and P. Habdas, *Europhys. Lett.* **115**, 68003 (2016).
- [4] M. Goldstein, *J. Chem. Phys.* **51**, 3728 (1969).
- [5] G. Adam and J. H. Gibbs, *J. Chem. Phys.* **43**, 139 (1965).
- [6] T. R. Kirkpatrick, D. Thirumalai, and P. G. Wolynes, *Phys. Rev. A* **40**, 1045 (1989).
- [7] F. Ritort and P. Sollich, *Adv. Phys.* **52**, 219 (2003).
- [8] T. R. Kirkpatrick and D. Thirumalai, *Rev. Mod. Phys.* **87**, 183 (2015).
- [9] D. Chandler, J. P. Garrahan, R. L. Jack, L. Maibaum, and A. C. Pan, *Phys. Rev. E* **74**, 051501 (2006).
- [10] L. Berthier, G. Biroli, J.-P. Bouchaud, W. Kob, K. Miyazaki, and D. R. Reichman, *J. Chem. Phys.* **126**, 184504 (2007).
- [11] S. Whitelam, L. Berthier, and J. P. Garrahan, *Phys. Rev. Lett.* **92**, 185705 (2004); G. Biroli and J. P. Garrahan, *J. Chem. Phys.* **138**, 12A301 (2013).
- [12] M. D. Ediger and P. Harrowell, *J. Chem. Phys.* **137** 080901 (2012).
- [13] T. L. Hill, *Statistical Mechanics* (McGraw-Hill, New York, 1956) chapt. 5; T. L. Hill, *J. Chem. Phys.* **23**, 617 (1955).
- [14] D. E. Stogryn and J. O. Hirschfelder, *J. Chem. Phys.* **31**, 1531, 1545 (1959).
- [15] Y. Singh, S. K. Deb, and A. K. Barua, *J. Chem. Phys.* **46**, 4036 (1967).
- [16] P. Harrowell, *Phys. Rev. E* **48**, 4359 (1993); D. N. Perera and P. Harrowell, *ibid* **54**, 1652 (1996).
- [17] J. P. Garrahan and D. Chandler, *Phys. Rev. Lett* **89**, 035704 (2002).
- [18] S. L. Singh, A. S. Bharadwaj, and Y. Singh, *Phys. Rev. E* **83**, 051506 (2011). The Ornstein-Zernike equation along with the Roger-Young (F. J. Rogers and D. A. Young, *Phys. Rev. A* **30**, 999 (1984) ) closure relation is found to give values of  $g(r)$  reasonably accurate in the fluid region. It however, fails to capture features such as the split second peak in the supercompressed region. Because of this we limit our calculation for  $\eta \leq 0.60$ . To check the accuracy we calculated value of  $Z = \frac{\bar{\beta}P}{\rho}$  at  $\eta = 0.597$  and found that the value is 24.2 which compares well with the exact value 25.3 .
- [19] P. N. Pusey and W. van Meegen, *Nature (London)* **320**, 340 (1986).
- [20] *Jamming and Rheology: Constrained Dynamics on Microscopic and Macroscopic Scales*, edited by A. J. Liu and S. R. Nagel (Taylor and Francis, New York, 2001).
- [21] A. Donev, F. H. Stillinger, and S. Torquato, *Phys. Rev. Lett* **96**, 225502 (2006).
- [22] V. A. Martinez, G. Bryant, and W. van Meegen, *Phys. Rev. Lett.* **101**, 135702 (2008); E. Zaccarelli, C. Valeriani, E. Sanz, W. C. K. Poon, M. E. Cates, and P. N. Pusey, *Phys. Rev. Lett.* **103**, 135704 (2009).
- [23] G. Parisi and F. Zamponi, *Rev. Mod. Phys.* **82**, 789 (2010).
- [24] J. P. Hansen and I. R. McDonald, *Theory of Simple Liquids*, 3rd ed. (Academic Press, Burlington, 2006).
- [25] W. Götze, *Complex Dynamics of Glass-Forming Liquids* (Oxford University Press, Oxford, 2009).
- [26] W. van Meegen, T. C. Mortensen, S. R. Williams, and J.

- Müller*, Phys. Rev. E **58**, 6073 (1998).
- [27] G. Brambilla, D. El Masri, M. Pierno, L. Berthier, L. Cipelletti, G. Petekidis, and A. B. Schofield, Phys. Rev. Lett. **102**, 085703 (2009); D. El Masri, G. Brambilla, M. Pierno, G. Petekidis, A. B. Schofield, L. Berthier, and L. Cipelletti, J. Stat. Mech. : Theo. and Expt., (2009) P07015.
- [28] L. Berthier and T. A. Witten, Phys. Rev. E **80**, 021502 (2009).
- [29] E. Zaccarelli, C. Valeriani, E. Sanz, W. C. K. Poon, M. E. Cates, and P. N. Pusey Phys. Rev. Lett. **103**, 135704 (2009).
- [30] P. N. Pusey, E. Zaccarelli, C. Valeriani, E. Sanz, W. C. K. Poon, and M. E. Cates, Phil. Trans. R. Soc. A **367**, 4993 (2009).
- [31] E. Zaccarelli, S. M. Liddle, and W. C. K. Poon, Soft Matter **11** 324 (2015).
- [32] D. Heckendorf, K. J. Mutch, S. U. Egelhaaf, and M. Laurati, Phys. Rev. Lett. **119**, 048003 (2017).
- [33] P. N. Segrè, S. P. Meeker, P. N. Pusey, and W. C. K. Poon, Phys. Rev. Lett. **75**, 958 (1995).